SECURITY INFORMATION

SECRET

Copy 4
RM L52G14

NACA RM L52G14

CONFIDENTIAL
SECURITY INFORMATION

JAN 6 1953

NACA

RESEARCH MEMORANDUM

CLASSIFICATION CHANGED

CONFIDENTIAL

To NACA Change

By authority of Form # 1350 per Hugh L. Dryden date Nov. 26, 52
per 12-18-52

PRELIMINARY RESULTS OF HORIZONTAL-TAIL LOAD MEASUREMENTS OF THE BELL X-5 RESEARCH AIRPLANE

By John T. Rogers and Angel H. Dunn

Langley Aeronautical Laboratory
Langley Field, Va.

CLASSIFIED DOCUMENT

This material contains information affecting the National Defense of the United States within the meaning of the espionage laws, Title 18, U.S.C., Secs. 793 and 794, the transmission or revelation of which in any manner to an unauthorized person is prohibited by law.

NATIONAL ADVISORY COMMITTEE FOR AERONAUTICS

WASHINGTON

August 15, 1952

SECRET CONFIDENTIAL
SECURITY INFORMATION

NATIONAL ADVISORY COMMITTEE FOR AERONAUTICS

RESEARCH MEMORANDUM

PRELIMINARY RESULTS OF HORIZONTAL-TAIL LOAD MEASUREMENTS OF THE BELL X-5 RESEARCH AIRPLANE

By John T. Rogers and Angel H. Dunn

SUMMARY

During the acceptance tests of the X-5 airplane made by Bell Aircraft Corp., measurements of the horizontal tail loads and static stability characteristics were obtained by the NACA High-Speed Flight Research Station. The results of the horizontal-tail load measurements are presented in this paper.

At Mach numbers of 0.50, 0.56, and 0.85 the trends of the balancing tail-load variation with increasing sweep angle from 20° to 59° were similar, with the largest down tail load occurring at a sweep angle of about 36° for each of these Mach numbers. The largest tail load in a down direction over the entire sweep range occurred at a Mach number of 0.85.

At 20° sweepback the tail load increased in a down direction as the indicated Mach number was increased from 0.54 to 0.84 during level flight.

During pull-ups at a Mach number of about 0.83 and at sweep angles of 20°, 45°, and 59°, the static longitudinal stability of the wing-fuselage combination was found to change at an airplane normal-force coefficient of approximately 0.3. The wing-fuselage aerodynamic center was found to move rearward as the sweep angle was increased from 20° to 59° throughout the normal-force-coefficient range covered in these tests. A larger change in the wing-fuselage aerodynamic center was experienced with sweep for the high normal-force-coefficient range than was experienced in the low normal-force-coefficient range.

INTRODUCTION

Acceptance tests of the X-5 airplane were conducted by Bell Aircraft Corp. at Edwards Air Force Base, Calif. and a preliminary evaluation of the horizontal-tail loads and static stability characteristics of the airplane was made by the NACA High-Speed Flight Research Station. Although these tests are not completed, it is felt that sufficient horizontal-tail-load information has been obtained at various wing sweep angles to be of general interest.

SYMBOLS

A	wing aspect ratio, (b^2/S)
$(a.c.)_{WF}$	aerodynamic center of wing-fuselage combination, percent M.A.C.
b	wing span, ft
b_{c_T}	wing span, based on equivalent tip chords, ft
c	chord at any section along the span, ft
c.g.	airplane center of gravity
C_{N_A}	airplane normal-force coefficient, nW/qS
C_{N_t}	tail normal-force coefficient, L_t/qS_t
$(C_{m_o})_{WF}$	wing-fuselage zero-lift pitching-moment coefficient, $M_o/qS\bar{c}$
c_s	chord at plane of symmetry, ft
c_t	tip chord (for rounded tips, c_t is the fictitious chord obtained by extending the leading and trailing edges to the extreme tip), ft
c_T	equivalent tip chord, length of a chord parallel to airplane line of symmetry, (between the leading edge and trailing edge extended), that forms one side of a trapezoid having an area equal to one-half the wing area, ft
$\left(\frac{dC_m}{dC_L}\right)_{WF}$	wing-fuselage static longitudinal stability parameter, $x/\bar{c}$
h_p	pressure altitude, ft

g acceleration due to gravity, ft/sec^2

l_t tail length, measured from airplane center of gravity to the quarter-chord station of the tail mean aerodynamic chord, ft

L_t aerodynamic horizontal-tail load, (up tail load positive, lb)

M Mach number

M.A.C., $\bar{c}$ mean aerodynamic chord, chord of an imaginary airfoil which throughout the normal flight range has the same force vectors as the three-dimensional wing, $\dfrac{\int_0^{b/2} c^2 dy}{\int_0^{b/2} c\ dy}$, ft

M_o zero-lift wing-fuselage pitching moment, ft-lb

n airplane normal acceleration, g units

q dynamic pressure, $\dfrac{\rho V^2}{2}$, lb/sq ft

S area of wing bounded by leading edge and trailing edge extended to the airplane line of symmetry disregarding fillets, $2\int_0^{b/2} c\ dy$, sq ft

S_t area of horizontal tail, sq ft

V free-stream velocity, ft/sec

W airplane gross weight, lb

x distance from aerodynamic center of wing-fuselage combination to airplane center of gravity, [positive if $(a.c.)_{WF}$ is forward of c.g.], ft

y lateral distance, ft

ρ mass density of air, slugs/cu ft

$\Lambda_{c/4}$ sweep angle of quarter chord of wing measured between the normal to the airplane line of symmetry and the quarter-chord line, deg

λ taper ratio, c_t/c_s

Subscript:

WF wing-fuselage combination

DESCRIPTION OF THE AIRPLANE

The Bell X-5 airplane is a research airplane incorporating a wing for which the angle of sweep can be varied in flight between 20° and 60° and is designed to investigate the transonic speed range. It is a single-place airplane powered by an Allison J-35-A-17 jet engine. Photographs of the airplane are given in figures 1 and 2 and a three-view drawing is presented in figure 3. All dimensions on the airplane are measured as a distance aft of fuselage station "0" shown in figure 3.

On the X-5 airplane as the wing sweep angle is varied, the wing pivots about the 38.02-percent chord at the wing root and also translates forward or rearward. Figure 4 shows the variation of wing pivot-point location measured as a distance aft of fuselage station "0" with wing sweep angle. The sweep limits indicated in this figure are 20.25° to 58.7° and these limits are controlled by limit switches on the airplane which prevent interference between the wing root and the fuselage fairings. The tolerance of these limit switches is about ±0.1° and changing the setting of the limit switches permits the minimum and maximum sweep limits to be changed. As also indicated in figure 4 the wing may be translated forward or aft 4.5 inches from the mean translation line without changing the wing sweep angle except at the end points. However, for these tests only the mean translation line was used in selecting combinations of wing sweep and translation.

As the wing sweep angle is changed, the wing dimensional characteristics change. These dimensional characteristics are plotted in figure 5 against wing sweep angle and are also given in table I which gives the airplane physical characteristics. All wing dimensional characteristics were defined by standard NACA methods.

As may be noted in figure 5, as the wing sweep angle is varied, the mean aerodynamic chord changes in length and position. This means that positions expressed in percent of the mean aerodynamic chord at the various sweep angles are not directly comparable. The center-of-gravity and aerodynamic-center positions defined in this paper are expressed in percent of the mean aerodynamic chord, and the center-of-gravity position is also expressed in table II as a fuselage station measured as a distance aft of fuselage station "0."

For these tests the slats were locked in the closed position.

INSTRUMENTATION AND ACCURACY

Standard NACA recording instruments are installed in the airplane to measure the following quantities:

- Airspeed
- Altitude
- Elevator stick force
- Normal, longitudinal, and transverse accelerations
- Pitching angular velocity and acceleration
- Rolling angular velocity
- Yawing angular velocity and acceleration
- Control positions
- Wing sweep angle

Shear and bending moments on the horizontal tail are measured by strain gages installed on the spar and skin at the root station 14.5 inches from the airplane center line as shown in figure 6. The outputs of these strain gages are recorded on a 36-channel recording oscillograph. Based on the results of static and flight loads evaluation, the estimated accuracy of the measured tail loads is ±75 pounds.

An NACA type A-6 total pressure head described in reference 1 was mounted on a nose boom approximately 1.1 maximum fuselage diameters forward of the nose of the airplane. The position error of the head was calibrated by the "fly-by" method up to $M = 0.70$ and above $M = 0.70$ by the radar phototheodolite method presented in reference 2. The estimated error in Mach number is about ±0.01.

Estimated errors of ±100 pounds in the weight determination and of ±0.02g in normal acceleration, in conjunction with the estimated Mach number error, result in an estimated error in the determination of the airplane normal-force coefficient of ±0.02.

For the demonstration tests the estimated error of the center-of-gravity location was about ±1.5 percent of the mean aerodynamic chord for all sweep angles.

METHODS

The total tail load outboard of the gage station was obtained from strain-gage measurements. This total load consists of aerodynamic and structural tail load. The tail loads presented are corrected for the inertia effects of the tail structure and therefore are aerodynamic tail loads.

In evaluating the tail loads, conditions were chosen in which the pitching acceleration was essentially zero. For zero pitching acceleration the tail load may be given by

$$L_t = \frac{nWx}{l_t + x} + \frac{\left(C_{m_o}\right)_{WF} qS\bar{c}}{l_t + x} \tag{1}$$

from which the solution for x may be obtained as follows:

$$x = \frac{\left(\frac{dL_t}{d_n}\right)(l_t)}{W - \frac{dL_t}{d_n}} \tag{2}$$

$$x = \frac{(l_t)\left(\frac{dC_{N_t}}{dC_{N_A}}\right)\left(\frac{S_t}{S}\right)}{1 - \left(\frac{dC_{N_t}}{dC_{N_A}}\right)\left(\frac{S_t}{S}\right)} \tag{3}$$

The wing-fuselage static longitudinal stability parameter $\left(\frac{dC_m}{dC_L}\right)_{WF}$ and the wing-fuselage combination aerodynamic-center location $(a.c.)_{WF}$ may be given by

$$\left(\frac{dC_m}{dC_L}\right)_{WF} = \frac{x}{\bar{c}} \qquad (4)$$

$$(a.c.)_{WF} = c.g. - \frac{x}{\bar{c}} \qquad (5)$$

RESULTS AND DISCUSSION

Shown in figure 7 is the variation of tail load expressed as tail normal-force coefficient C_{N_t}, with sweep angle at Mach number of 0.50, 0.56, and 0.85 with the center of gravity located at about fuselage station 155. As the wing sweep angle is changed, the center-of-gravity location shifts, but this shift is less than the estimated error in the center-of-gravity determination. The data were obtained during wing sweep changes at an altitude of approximately 20,000 feet. At the Mach numbers tested the peak down tail load occurred at a sweep angle of about 36° and the general trends of the tail-load variation with sweep angle at the various Mach numbers are similar. At $M = 0.85$ only a small increase in down tail load occurred as the sweep angle was increased from 20° to 36°; whereas at the lower Mach numbers a larger increase in down tail load occurred for this sweep change. At all sweep angles the largest down tail load occurred at $M = 0.85$.

Data obtained during level-flight trim points at 20° sweepback at an approximate altitude of 24,000 feet and average weight of about 8,800 pounds are shown on figure 8. This level-flight altitude corresponded to a change in airplane normal-force coefficient from 0.36 at $M = 0.54$ to 0.13 at $M = 0.84$. The tail load increased in a down direction as the Mach number was increased from 0.54 to 0.84. Sufficient data are not available to determine the effect of center-of-gravity location and normal-force coefficient on tail loads in order that data of figures 7 and 8 be combined.

Figure 9 shows the variation of tail load, expressed as tail normal-force coefficient C_{N_t}, with airplane normal-force coefficient C_{N_A} during a series of pull-ups at a Mach number of about 0.83 at altitudes of 20,000 and 30,000 feet and at sweep angles of 20°, 45°, and 59°. At normal-force coefficients near 0.3 the slope (dC_{N_t}/dC_{N_A}) changed at each of the three sweep angles tested. This change in the slope indicates a change in the stability of the wing-fuselage combination caused by a movement of the wing-fuselage aerodynamic center $(a.c.)_{WF}$. For 20° sweepback and with the center of gravity located at approximately 23.1 percent of the mean aerodynamic chord at $M \approx 0.83$, the wing-fuselage combination is stable at normal-force coefficients below 0.3 but becomes unstable at the higher normal-force coefficients. At a sweep angle of 45° and with the center of gravity located at approximately 30.4 percent of the mean aerodynamic chord the wing-fuselage combination is stable at normal-force coefficients below 0.3 but experiences a reduction in stability at higher normal-force coefficients. For a sweep angle of 59° and with the center of gravity located at 44.7 percent of the mean aerodynamic chord the wing-fuselage combination is unstable at normal-force coefficients below 0.2 and becomes stable at normal-force coefficients above about 0.3.

The slopes (dC_{N_t}/dC_{N_A}) of the data presented in figure 9 were determined by the least-squares method. The distance from the aerodynamic center to the center of gravity x, the static longitudinal stability parameter $(dC_m/dC_L)_{WF}$, and the aerodynamic center of the wing-fuselage combination $(a.c.)_{WF}$ were determined from the slopes (dC_{N_t}/dC_{N_A}) and from equations (3) to (5) and are summarized in table II.

The values of wing-fuselage aerodynamic center $(a.c.)_{WF}$ summarized in table II are also shown in figure 10 as variations with wing sweep angle. For the normal-force-coefficient range covered in these tests the aerodynamic center of the wing-fuselage combination moves rearward as the sweep angle is increased from 20° to 59° at $M \approx 0.83$. As may be noted in figure 10, a larger change in the wing-fuselage aerodynamic center is experienced with sweep for the high normal-force-coefficient range than was experienced in the low normal-force-coefficient range.

CONCLUSIONS

From the horizontal-tail-load measurements obtained during the Bell acceptance tests of the X-5 airplane it has been shown that:

1. During sweep changes at an altitude of 20,000 feet, the trends of the balancing tail load variation with sweep angle at Mach numbers of 0.50, 0.56, and 0.85 were similar with the largest down tail load occurring at approximately 36° sweep angle at each Mach number tested. The largest balancing tail load in a down direction over the entire sweep range from 20° to 59° occurred at a Mach number of 0.85.

2. During level-flight-trim points at 20° sweepback at an altitude of about 24,000 feet and an airplane weight of about 8,800 pounds, the tail load increased in a down direction as the Mach number was increased from 0.54 to 0.84.

3. During pull-ups at a Mach number of about 0.83 and at sweep angles of 20°, 45°, and 59°, the wing-fuselage combination was stable at 20° and 45° sweepback and unstable at 59° sweepback at normal-force coefficients less than 0.3. At normal-force coefficients near 0.3 the stability of the wing-fuselage combination changed for these sweep angles, became unstable at a sweep angle of 20°, experiencing a reduction in stability at 45°, and became stable at 59° as the normal-force coefficient increased. For the normal-force-coefficient range covered in these tests the aerodynamic center of the wing-fuselage combination moved rearward as the sweep angle was increased from 20° to 59°. A larger change in the wing-fuselage aerodynamic center was experienced with sweep for the high normal-force-coefficient range than was experienced for the low normal-force-coefficient range.

Langley Aeronautical Laboratory,
National Advisory Committee for Aeronautics,
Langley Field, Va.

REFERENCES

1. Gracey, William, Letko, William, and Russell, Walter R.: Wind-Tunnel Investigation of a Number of Total-Pressure Tubes at High Angles of Attack. Subsonic Speeds. NACA TN 2331, 1951. (Supersedes NACA RM L50G19.)

2. Zalovcik, John A.: A Radar Method of Calibrating Airspeed Installations on Airplanes in Maneuvers at High Altitudes and at Transonic and Supersonic Speeds. NACA Rep. 985, 1950. (Supersedes NACA TN 1979.)

REFERENCES

1. Gracey, William, Letko, William, and Russell, Walter R.: Wind-Tunnel Investigation of a Number of Total-Pressure Tubes at High Angles of Attack. Subsonic Speeds. NACA TN 2331, 1951. (Supersedes NACA RM L50G19.)

2. Zalovcik, John A.: A Radar Method of Calibrating Airspeed Installations on Airplanes in Maneuvers at High Altitudes and at Transonic and Supersonic Speeds. NACA Rep. 985, 1950. (Supersedes NACA TN 1979.)

TABLE I.- PHYSICAL CHARACTERISTICS OF THE BELL X-5 AIRPLANE

Airplane:			
Weight during acceptance tests:			
Full fuel, lb			9850
Less fuel, lb			7740
Power plant:			
Axial-flow turbojet engine			J-35-A-17
Guaranteed rated thrust at 7800 rpm and static sea-level conditions, lb			4900
Horizontal distance from fuselage station zero to 0.25 mean aerodynamic chord of horizontal tail, in.			355.6
Wing:			
Airfoil section (perpendicular to 38.02 percent chord line):			
Root			NACA $64_{(10)}$A011
Tip			NACA $64_{(08)}$A008.28
Sweepback angle (0.25 local chord), deg	20	45	60
Area, sq ft	167.0	172.3	186.7
Span, ft	31.9	24.8	19.7
Span between equivalent tips, ft	30.9	24.4	18.7
Aspect ratio	6.09	3.56	2.08
Taper ratio	0.435	0.440	0.406
Mean aerodynamic chord, ft	5.61	7.37	10.35
Location L.E. mean aerodynamic chord (fuselage station)	139.9	127.5	96.8
Incidence root chord, deg	0	0	0
Dihedral, deg	0	0	0
Geometric twist	0	0	0
Horizontal tail:			
Airfoil section			NACA 65A006
Area, sq ft			31.5
Span, ft			9.56
Aspect ratio			2.9
Maximum elevator displacement, deg			
Up			25
Down			20
Sweepback angle at 0.25 percent chord, deg			45
Mean aerodynamic chord, in.			42.8
Vertical tail:			
Airfoil section			NACA 65A006
Area, sq ft			29.5
Span, ft			6.25
Aspect ratio			1.32
Maximum rudder displacement, deg			±35

NACA

TABLE II.- SUMMARY OF STATIC LONGITUDINAL STABILITY OF X-5 AIRPLANE

OBTAINED FROM TAIL-LOAD MEASUREMENTS DURING PULL-UPS

[$M \approx 0.83$]

Angle of sweep, Λ, deg	C_{N_A} range	c.g. location, fuselage station	$\frac{dC_{N_t}}{dC_{N_A}}$	x, ft	M.A.C., ft	Values expressed in terms of M.A.C.: c.g. location, percent M.A.C.	Values expressed in terms of M.A.C.: $\left(\frac{dC_m}{dC_L}\right)_{WF}$	Values expressed in terms of M.A.C.: $(a.c.)_{WF}$, percent M.A.C.
20	<0.3	155.4	-0.0646	-0.201	5.61	23.1	-0.036	26.7
20	>.3	155.4	.0981	.303	5.61	23.1	.055	17.6
45	<.3	154.5	-.0463	-.141	7.37	30.4	-.019	32.3
45	>.3	154.5	-.0237	-.073	7.37	30.4	-.010	31.4
59	<.2	153.9	.0786	.225	10.05	44.7	.023	42.4
59	>.3	153.9	-.1929	-.539	10.05	44.7	-.054	50.1

NACA

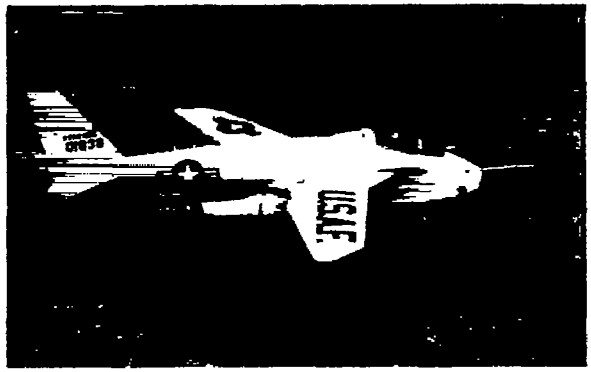

(a) 20° sweepback. NACA LAL 72819

(b) 45° sweepback. NACA LAL 72820

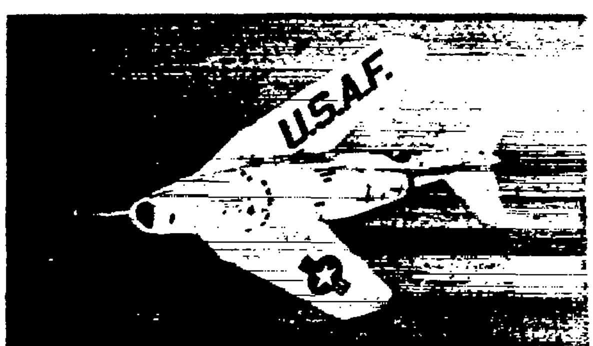

(c) 60° sweepback. NACA LAL 72821

Figure 1.- Photographs of the Bell X-5 airplane in flight.

[redacted]
SECURITY INFORMATION

Figure 2.- Photograph of Bell X-5 airplane in landing configuration.

[redacted]
SECURITY INFORMATION

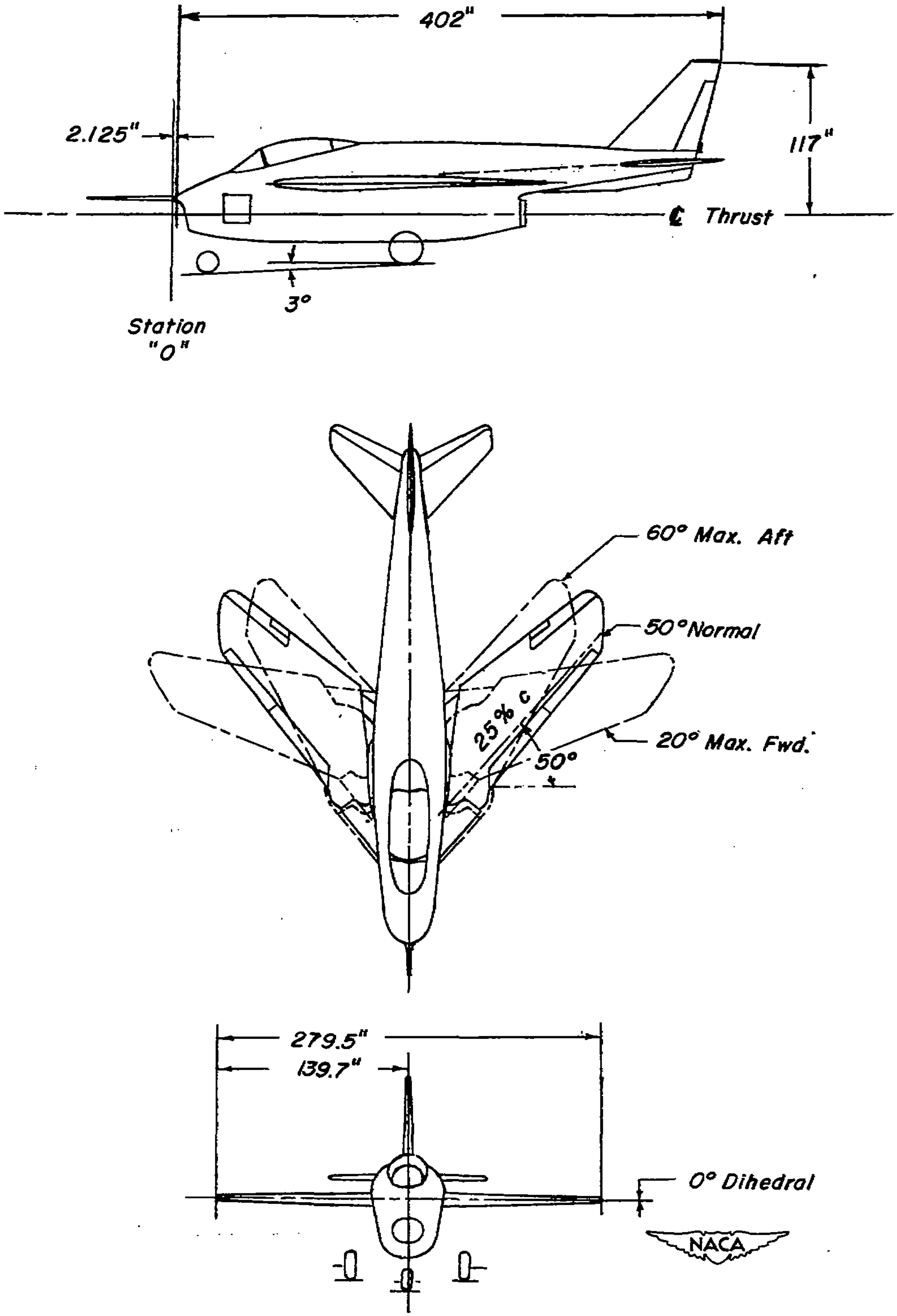

Figure 3.- Three-view drawing of the Bell X-5 airplane.

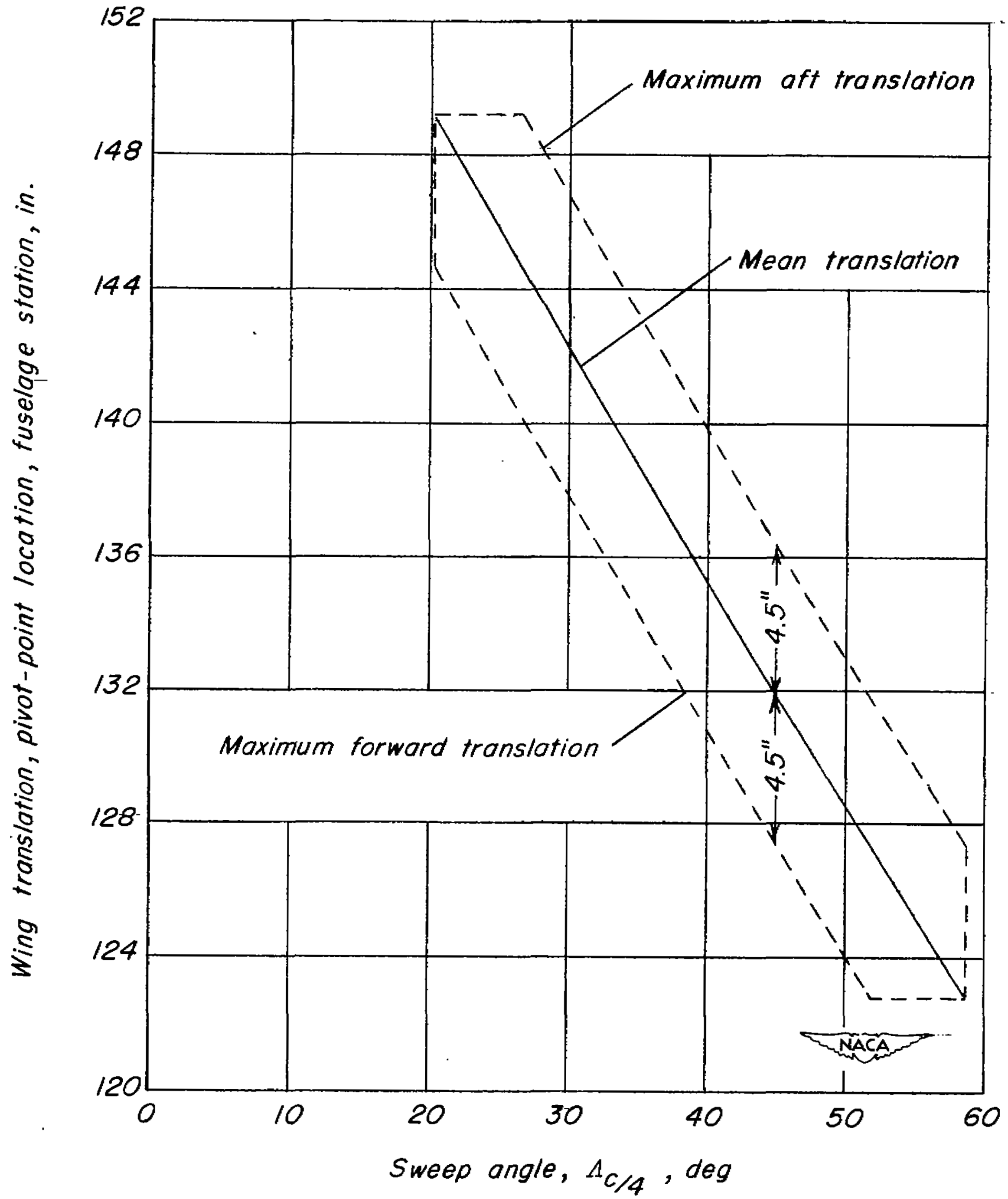

Figure 4.- Wing pivot-point location plotted against wing sweep angle X-5 airplane.

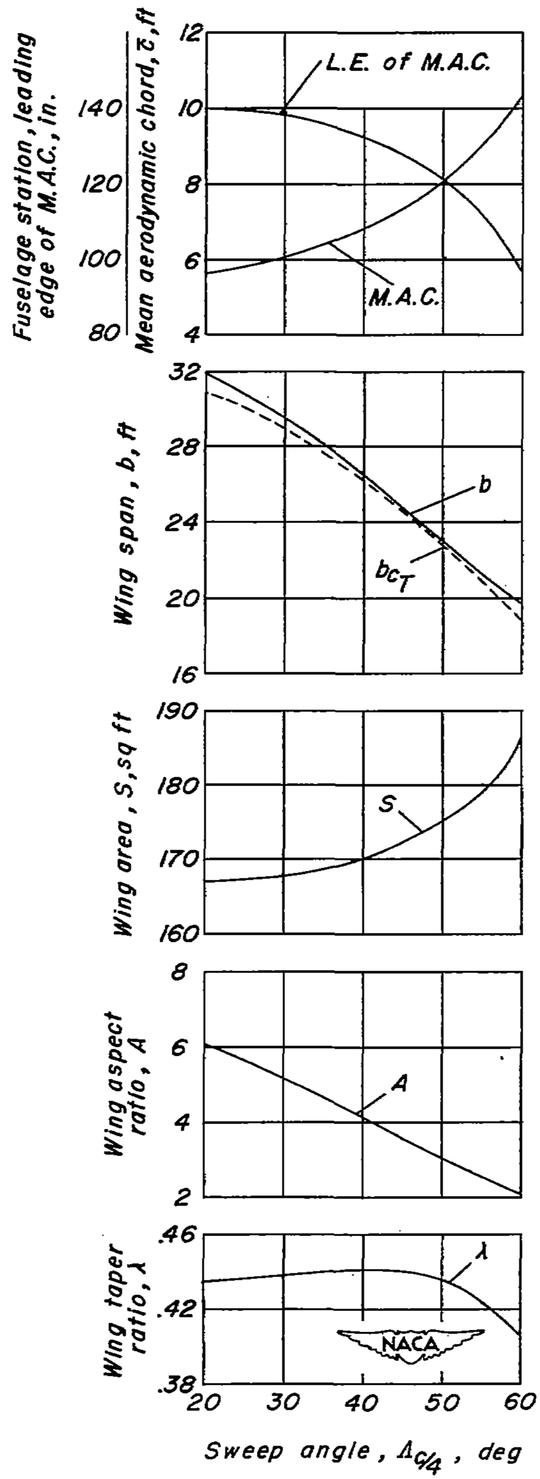

Figure 5.- Dimensional characteristics of X-5 airplane plotted against wing sweep angle.

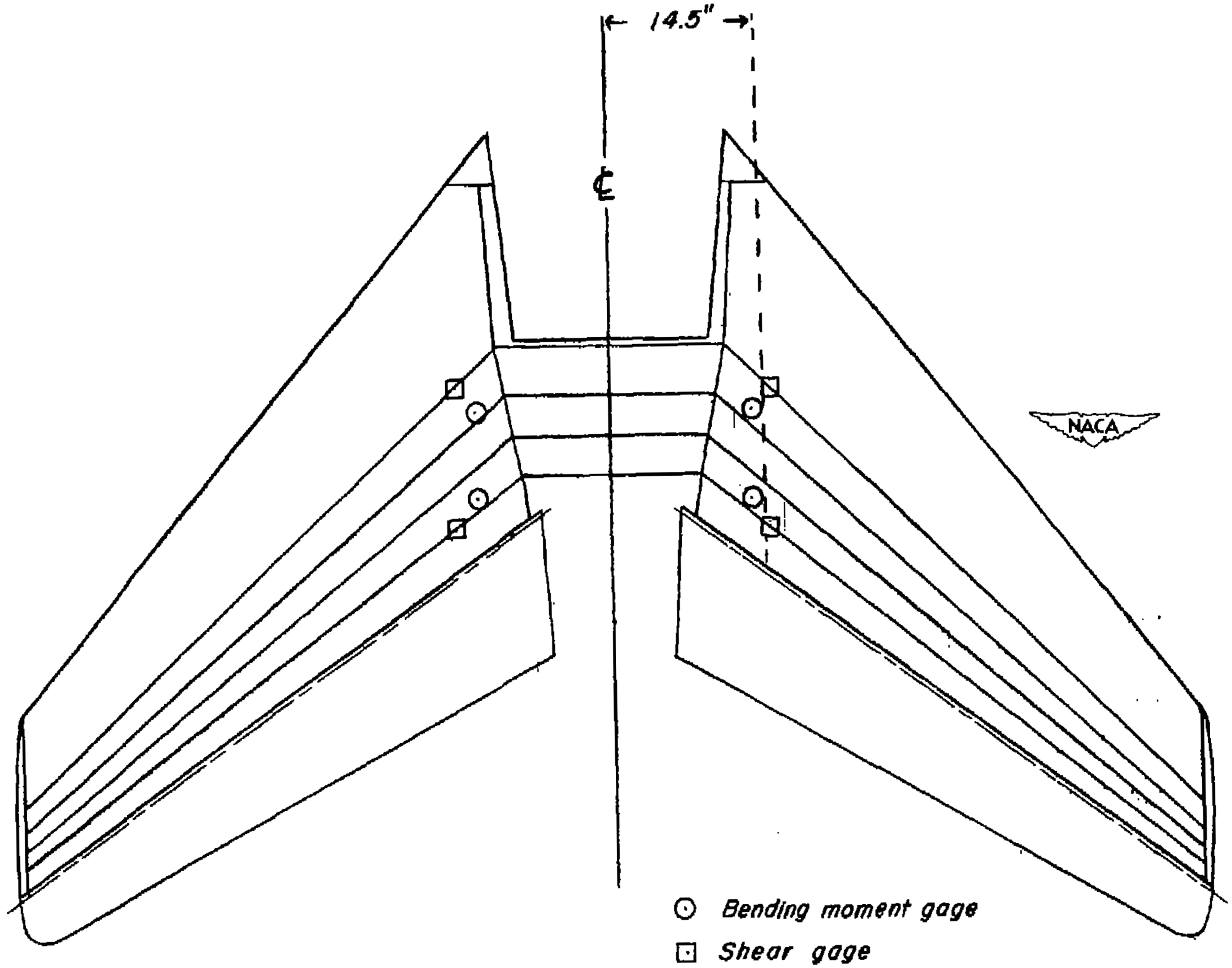

Figure 6.- Horizontal tail of X-5 airplane showing the location of the strain gages.

[redacted]
SECURITY INFORMATION

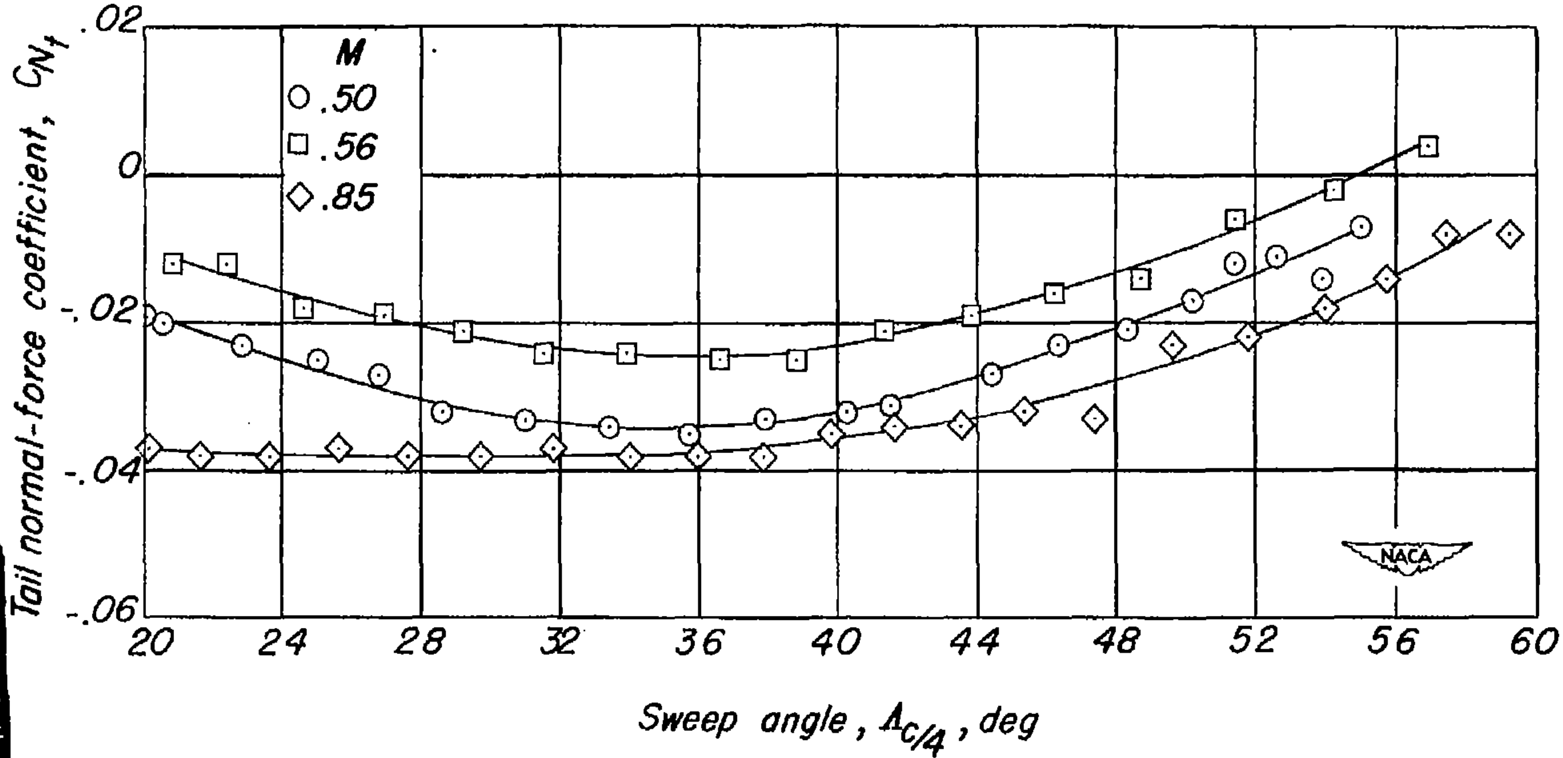

Figure 7.- Variation of tail normal-force coefficient with sweep angle for level flight. $h_p \approx$ 20,000 feet; W $\approx$ 8,500 pounds; c.g. $\approx$ fuselage station 155.0.

[redacted]
SECURITY INFORMATION

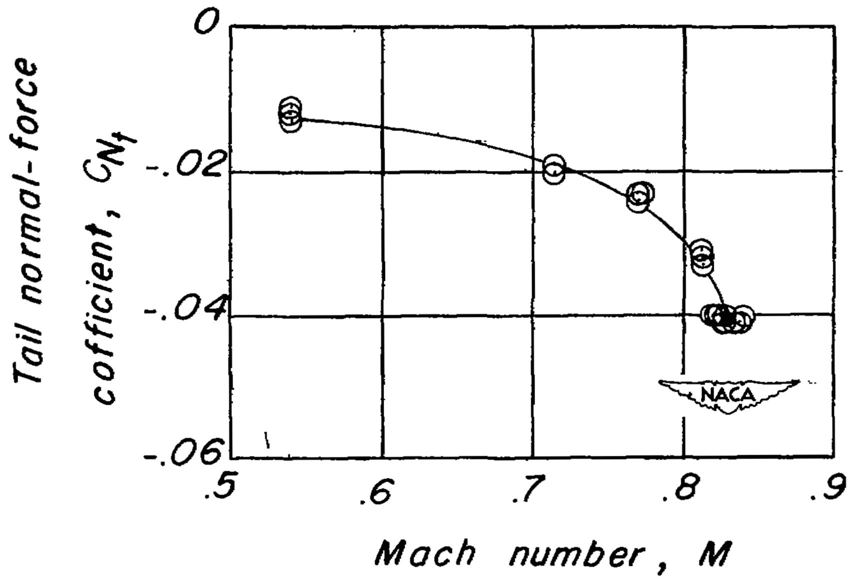

Figure 8.- Variation of tail normal-force coefficient with Mach number during level flight. $\Lambda = 20^{\circ}$; $h_p \approx 24,000$ feet; $W \approx 8,800$ pounds; c.g. $\approx$ fuselage station 155.4.

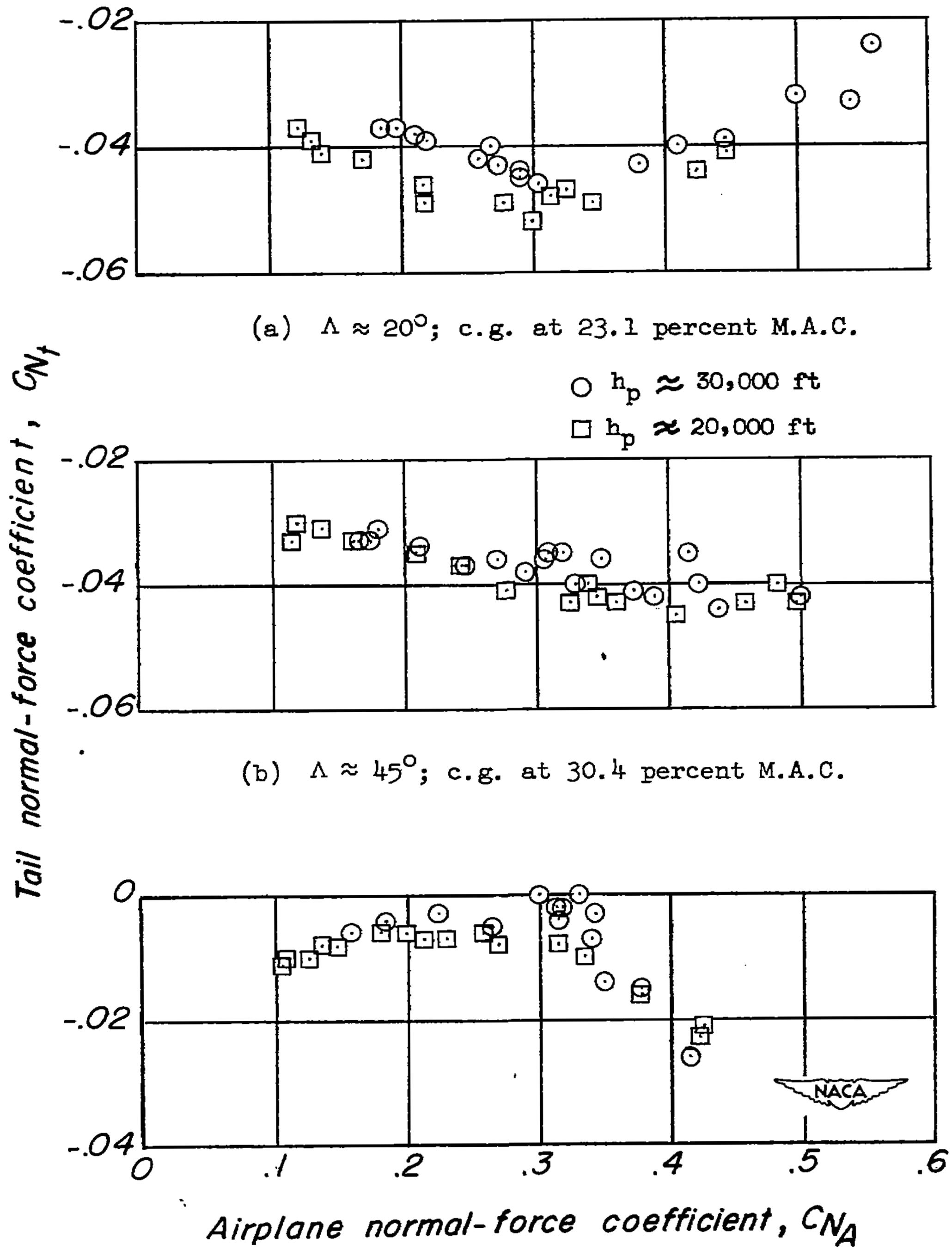

(a) $\Lambda \approx 20^{\circ}$; c.g. at 23.1 percent M.A.C.

(b) $\Lambda \approx 45^{\circ}$; c.g. at 30.4 percent M.A.C.

(c) $\Lambda \approx 59^{\circ}$; c.g. at 44.7 percent M.A.C.

Figure 9.- Variation of tail normal-force coefficient with airplane normal-force coefficient during pull-ups. $M \approx 0.83$.

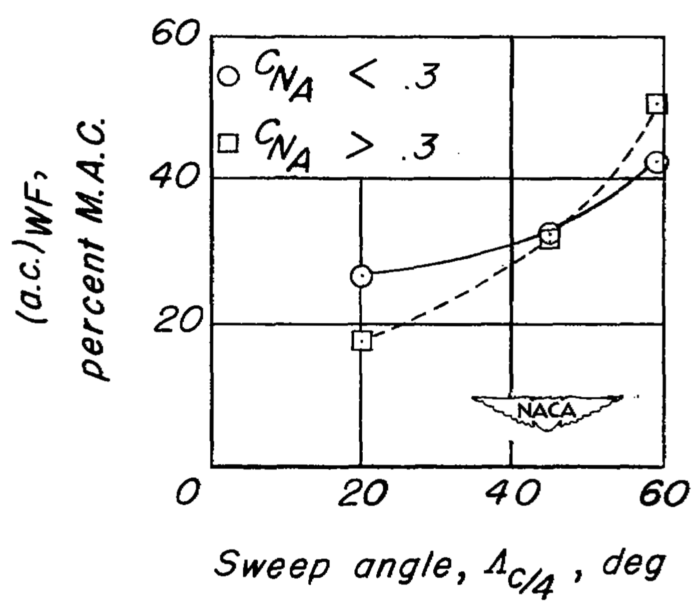

Figure 10.- Variation of wing-fuselage aerodynamic center with wing sweep angle for $M \approx 0.83$.

INDEX

ABSTRACT

Horizontal-tail load measurements were made during the Bell acceptance tests of a transonic speed research airplane having wings variable in flight between 20° and 60° sweepback. Load measurements were made during sweep changes in level flight from Mach numbers of 0.50 to 0.85, and during pull-ups at a Mach number of 0.83 at sweep angles of 20°, 45°, and 59°.

[redacted]

[redacted] [redacted]